Influence of random fluctuations on delayed bifurcations: The case of additive white noise

N. G. Stocks, R. Mannella,* and P. V. E. McClintock

Department of Physics, University of Lancaster, Lancaster LA1 4YB, United Kingdom

(Received 19 June 1989)

The influence of additive white noise on the delay of a bifurcation point in the presence of a swept control parameter has been studied by analog experiment and digital simulation. Measurements of the time taken for the second moment $\langle x^2(t) \rangle$ to reach a given threshold are in excellent agreement with the calculations of Zeghlache, Mandel, and Van den Broeck [Phys. Rev. A **40**, 286 (1989)]. It is demonstrated, however, that the mean first-passage time (MFPT) for $x^2(t)$ to attain the same threshold, corresponding to the quantity that is usually determined in laser experiments, can be markedly different. It may be either larger or smaller, depending on the conditions under which the measurements are made. A calculation of the MFPT is presented and shown to be in excellent agreement with the experimental measurements and to reduce, in the relevant limit, to the theoretical results previously published by Torrent and San Miguel [Phys. Rev. A **38**, 245 (1988)].

I. INTRODUCTION

Nonlinear dynamical systems respond to random fluctuations (noise) in diverse and often unexpected ways.[1-3] Of particular interest and importance are the noise-driven phenomena that occur near instability points of the deterministic (noise-free) system, which have been the subject of numerous investigations, both experimental and theoretical. One way of studying such effects is by changing a control parameter through the critical value at which an initially stationary state suddenly becomes unstable and the system bifurcates, an obvious physical example being the single-mode laser in the good cavity limit as the optical-pump parameter is increased past the first lasing threshold. In situations of this kind, the relevant control parameter can either be switched discontinuously[4-9] or it can be swept,[10-20] usually at a constant rate, through the transition.

In cases where the control parameter is swept, it is typically found that the bifurcation point is *postponed* as compared to that corresponding to quasistatic changes. In a recent paper Zeghlache, Mandel, and Van den Broeck[19] (ZMVB) have calculated the magnitude of this postponement for a variety of initial conditions under the influence of a wide range of intensities and types of noise. The main purposes of the present paper are, first, to report the results of analog experiments and digital simulations undertaken to test the validity and applicability of the ZMVB approach for the particular case of additive, white, Gaussian noise. Second, based on the ideas of Torrent and San Miguel[20] (TSM) we extend the analysis to encompass a different definition of the postponement, in terms of the mean first-passage time (rather than the time evolution of a moment) which, arguably, provides a more natural comparison with the quantities usually measured in experiments. The theoretical results obtained in this way are also tested by analog experiment and digital simulation.

In Sec. II we set out in more detail the problem that is being addressed, we summarize the salient features of the ZMVB theory, and we show how their calculations may be extended to give a measure of the postponement based on the mean first-passage time (MFPT) recovering, in a limiting case, the theoretical results of TSM. In Sec. III we describe and discuss tests of the theory, in which we compare the results of analog experiments and digital simulations with theoretical predictions calculated by the methods discussed in Sec. II. Finally, in Sec. IV we summarize the most important results of the investigations and draw conclusions.

II. THEORY

A. Statement of the problem

Following ZMVB, we consider the evolution of the system

$$\dot{x} = \mu(t)x + \eta(t) , \tag{2.1}$$

$$\mu(t) = \mu(0) + vt , \tag{2.2}$$

where $\mu(0) < 0$ and $v > 0$, and the additive noise term $\eta(t)$ satisfies

$$\tau\dot{\eta} = -\eta + \xi(t) \tag{2.3}$$

in which τ is the correlation time of the noise and $\xi(t)$ is a Gaussian white-noise source defined by

$$\langle \xi(t) \rangle = 0, \quad \langle \xi(t)\xi(t') \rangle = 2D\delta(t - t') . \tag{2.4}$$

In the present paper, we restrict ourselves to the particular case of white noise, so that the correlation time τ is zero; the more general case of colored ($\tau > 0$) noise will be considered separately in a future paper. A very large class of nonlinear systems can, of course, be represented by the simple form (2.1) close to their bifurcation points, by linearizing around the trivial (zero-amplitude) solu-

tion. In the particular case of the laser, x is related to the electric field amplitude and $\mu(t)$ to the optical pump parameter, as discussed by ZMVB.

The physical consequences for the system (2.1) of sweeping the parameter $\mu(t)$ according to (2.2) are most easily appreciated by consideration of the equivalent (time-dependent) potential, sketched in Fig. 1. The important features are that to start with, for $\mu(t) < 0$, the potential possesses a minimum at $x = 0$ which, however, grows ever shallower with the passage of time until, when $\mu(t)$ passes zero at $t = \bar{t}$ and becomes positive, the potential exhibits a maximum at $x = 0$ instead of a minimum; correspondingly, of course, the $x = 0$ solution becomes unstable at $t = \bar{t}$ and any perturbation, however small, will then be sufficient to push the system away towards rapidly growing positive or negative x.

For quasistatic changes, the bifurcation point of the system occurs when $\mu = 0$. When the system is swept according to (2.2), on the other hand, it is clear that the value of μ at which a given $|x|$ is reached will depend on the starting conditions and, in general, upon the speed v with which μ is increased. Of course, if the initial value of x is zero then, in the absence of noise ($D = 0$), the system will *never* leave the $x = 0$ solution, even in the unstable region when $\mu > 0$ at $t > \bar{t}$, as indicated by trajectory a in Fig. 1. In physically interesting situations, however, the initial value of x will be nonzero and there will also be some noise. If the initial value of $x = x(0)$ then, still keeping $D = 0$, it can be shown[13] that the time t^* for the

swept system to bifurcate, as defined by $x^2(t)$ attaining an arbitrary threshold x_{th}^2 for $\mu > 0$, is given exactly by $t^* = 2\bar{t}$ for the particular case where $x_{th}^2 = x^2(0)$: the corresponding trajectory of $x(t)$ is indicated by the curve b in Fig. 1. [The independence of $t^* = 2\bar{t}$ on the sweep velocity v seems at first sight astonishing. It is, however, intuitively quite plausible in the following sense. The smaller v becomes, the closer the system will have approached to $x = 0$ when the static bifurcation point is reached at $\mu = 0$; and the longer, therefore, it will take a leave the vicinity of $x = 0$ and attain $x(0)$ again after the potential has inverted for $\mu > 0$. Thus it is perfectly reasonable that t^* should increase in just the same way as $\bar{t}$ as the result of a decrease in v, such that their ratio remains constant.]

The problem considered by ZMVB, to which we now address ourselves in detail, is the question of what happens to t^* in the presence of noise, i.e., when $D \neq 0$ in (2.4). First, we note that the definition of t^* used for the deterministic case is no longer adequate, because each repetition of the experiment will yield a different $x(t)$ trajectory: a new definition of t^* based on averaged quantities is clearly required. The definition adopted by ZMVB is that t^* in the noisy system should be the time taken for the second moment $\langle x^2(t) \rangle$ to reach the threshold value x_{th}^2, which is now not necessarily equal to $x(0)$ but discussed in terms of the dimensionless number $\alpha = x_{th}^2/x^2(0)$ where $\alpha \geq 1$ (see below). Here, $x(0)$ is the fixed initial condition at $t = 0$ for the "external noise" case, where the noise is applied at the start of the sweep. For the "internal noise" case, where the noise is applied continuously and the system is allowed to reach a stationary state for $\mu = \mu(0)$ prior to commencement of the sweep, $x^2(0)$ is replaced by its average value $\langle x^2(0) \rangle$. The values of t^* calculated by ZMVB for these two kinds of initial conditions are, of course, different. In Sec. II B below we review briefly the ZMVB arguments and their most important conclusions.

An alternative definition of t^*, however, following TSM, is that it should be the *average time* taken for the system to reach x_{th}^2; we would argue that in many cases it corresponds more closely to what is usually measured in experiments. This definition is identical to the mean first-passage time between $x^2(0)$ and x_{th}^2 in the case of external noise, and can be regarded as an effective MFPT between $\langle x^2(0) \rangle$ and x_{th}^2 for the internal noise case. In Sec. II C we show how t^*, defined in this different way, may be calculated for both internal and external additive white noise.
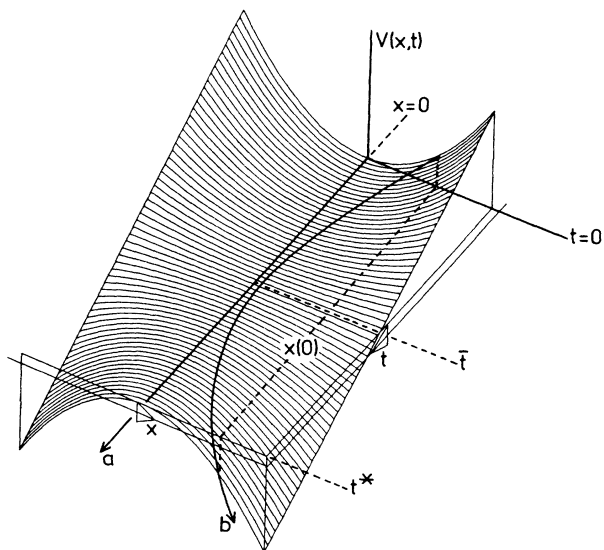

FIG. 1. Sketch of the time-dependent potential $V(x,t)$ corresponding to Eqs. (2.1) and (2.2) in the absence of fluctuations, i.e., with $D = 0$ in (2.4). If the system could be started *exactly* at $x = 0$ at $t = 0$, then its $x(t)$ trajectory would in principle remain at $x = 0$ even in the unstable region for $t > t$ (curve a). If, instead, the system is started at $x = x(0)$ at $t = 0$, it will approach $x = 0$ until $t = \bar{t}$ and then diverge away again for $t > \bar{t}$, passing to $x = x(0)$ when $t = t^* = 2\bar{t}$ (see Ref. 13).

B. ZMVB theory of the postponement

As already indicated, ZMVB theory distinguishes carefully between the two cases: internal noise (where the system is prepared in contact with the noise source) and external noise [where the system is prepared at $x(0)$ for each sweep and the noise is added only at the start of the sweep itself]. Referring to Eqs. (2.1)–(2.4), they introduce the quantities

$$\alpha = \frac{x_{\text{th}}^2}{\langle x^2(0) \rangle} \ ,$$

$$b = \frac{D}{x^2(0)} \left[\frac{\pi}{v} \right]^{1/2} \ ,$$

$$\beta = \frac{D}{x_{\text{th}}^2} \left[\frac{\pi}{v} \right]^{1/2} \ ,$$

$$a = \frac{\mu(0)}{\sqrt{v}} \ ,$$

$$z = \frac{\mu(0) + vt^*}{\sqrt{v}} \ ,$$

$$c = \frac{1}{\tau \sqrt{v}} \ .$$

(2.5)

The formal solution of (2.1) is

$$x(t) = x(0) \exp \left[\int_0^t \mu(s) ds \right] + \int_0^t \exp \left[\int_s^t \mu(y) dy \right] \xi(s) ds \ .$$

(2.6)

ZMVB now consider the average quantities

$$\langle x(t) \rangle = \langle x(0) \rangle \exp \left[\int_0^t \mu(s) ds \right]$$

(2.7a)

and

$$\langle x^2(t) \rangle = \exp \left[\int_0^t \mu(s) ds \right] \left[\langle x^2(0) \rangle + 2 \int_0^t \langle x(0) \eta(s) \rangle \exp \left[-\int_0^s \mu(y) dy \right] ds \right.$$

$$\left. + \int_0^t \int_0^t \langle \eta(s) \eta(p) \rangle \exp \left[-\int_p^s \mu(y) dy \right] ds \, dp \right] \ .$$

(2.7b)

For present purposes, it is Eq. (2.7b) that is of relevance. The stochastic integrals on the right-hand side can easily be evaluated and it is possible to solve the resulting equation for t^*, i.e., for the value of t at which $\langle x^2(t) \rangle$ reaches the predetermined threshold x_{th}^2. For the external noise case [remembering that z is related to t^* via Eq. (2.5)] ZMVB find that we should search for the roots of

$$\alpha e^{-z^2} - e^{-a^2} - \sqrt{2} bce^{c^2} \int_a^z ds \exp \left[-\frac{(s+c)^2}{z} \right] \left[\text{erf} \left[\frac{s-c}{\sqrt{2}} \right] - \text{erf} \left[\frac{a-c}{\sqrt{2}} \right] \right] = 0 \ ,$$

(2.8)

where $\text{erf}(x)$ is the usual error function.[21] For the internal noise case, noting that

$$\langle x^2(0) \rangle = \frac{D}{\mu(0)[\mu(0)\tau - 1]} \ , \quad \langle x(0)\eta(t) \rangle = \frac{D}{\mu(0)} e^{-|t|/\tau} \ , \quad \langle \eta(0)\eta(t) \rangle = \frac{D}{\tau} e^{-|t|/\tau} \ ,$$

(2.9)

ZMVB find

$$\frac{1}{\beta} e^{-z^2} - \frac{c}{(a^2 - ac)\sqrt{\pi}} e^{-a^2} - \frac{\sqrt{2}c}{c-a} e^{-a^2} \exp \left[-\frac{(a+c)^2}{2} \right] \left[\text{erf} \left[\frac{z+c}{\sqrt{2}} \right] - \text{erf} \left[\frac{a+c}{\sqrt{2}} \right] \right]$$

$$- \sqrt{2}ce^{c^2} \int_a^z ds' \exp \left[-\frac{(s+c)^2}{2} \right] \left[\text{erf} \left[\frac{s-c}{\sqrt{2}} \right] - \text{erf} \left[\frac{a-c}{\sqrt{2}} \right] \right] = 0 \ . \quad (2.10)$$

Here, in a similar way, z should be searched for as the root of (2.10).

C. "Mean first-passage time" approach

As it is clear from the previous discussion, the ZMVB results are obtained by consideration of the quantity $\langle x^2(t) \rangle$. In a physical system similar to a laser, for example, this approach corresponds to signal-averaging the intensity $x^2(t)$ while the pump parameter is being swept through the bifurcation, and asking the question: What

is the value of the pump parameter when this average crosses a predefined threshold x_{th}^2? However, it is also possible to ask a slightly different question, namely: what is the value of the pump parameter at which, on average, the laser intensity $x^2(t)$ crosses a given threshold x_{th}^2? In contrast to the previous case, we find the value of the pump parameter for which $x^2(t) = x_{\text{th}}^2$ *for each individual realization*; then we average over many realizations to determine the MFPT. This is the idea underlying the TSM approach. Due to the nonlinear relation between x and t (and implicitly the pump parameter) these two

averaging procedures will, in general, lead to two different results.[22] Figure 2 (obtained experimentally by analog simulation, as explained in Sec. III) clarifies the argument: we have plotted the probability distribution of $x^2(t)$ as a function of t. The ZMVB average corresponds to taking the average along the x^2 axis, at t^* [Fig. 3(a)], the MFPT average corresponds to taking the average along the t axis, at x_{th}^2 [Fig. 3(b)]. As it is clear from Fig. 3(a), the tail $P(x^2, t^*)$ for large x^2 will yield a $t^*(t_{ZMVB}^*)$ that is larger than the t^* obtained via the MFPT average (t_{MFPT}^*).

If the static Kramers escape rate to x_{th}^2 can be discarded (where by "static" we mean the activation rate due

solely to the stochastic force, not due to the inherent instability above threshold), it is possible to obtain $P(x^2, t)$ and t_{MFPT}^* by means of a semianalytical method: the idea is to evaluate the stochastic integral appearing in Eq. (2.6) with the appropriate distribution for $x(0)$ and to find the value $t = t_{MFPT}^*$ for which (2.6) is satisfied. In the external noise case we are led to compute the solution of

$$x_{th}^2 - \exp[2\mu(0)t^* + vt^{*2}][x(0) + \sqrt{F(t^*)}y_1]^2 = 0 ,$$
$$(2.11)$$

where y_1 is a Gaussian variable with standard deviation one and average zero. $F(t)$ is given by

$$F(t) = \int_0^t \int_0^t \exp\left[-\mu(0)s - \frac{vs^2}{2} - \mu(0)y - \frac{vy^2}{2}\right] \langle \eta(s)\eta(y) \rangle ds \, dy$$

$$= \frac{D}{\tau}\left[\frac{2\pi}{v}\right]^{1/2} \int_0^t \exp\left[-\frac{vy^2}{2} - y\left[\frac{1}{\tau} + \mu(0)\right]\right]\left[\text{erf}\left[\frac{\sqrt{v}y + a - c}{\sqrt{2}}\right] - \text{erf}\left[\frac{a - c}{\sqrt{2}}\right]\right] . \qquad (2.12)$$

Equation (2.11) follows from

$$\int_0^t \exp\left[-\mu(0)s - \frac{v^2}{2}s^2\right]\eta(s)ds \equiv \sqrt{F(t)}y_1 \qquad (2.13)$$

because the integral appearing on the left-hand side of (2.13), a linear combination of Gaussian variables, can be written as a single Gaussian variable y_1 with the appropriate standard deviation $F(t)$.

Similarly for the case of internal noise, keeping in mind that we must also satisfy Eq. (2.9), it is possible to derive

$$x_{th}^2 - \exp[2\mu(0)t^* + vt^{*2}]\left\{y_1\left[\left[\frac{D}{\mu(0)(\tau - 1)}\right]^{1/2} + G(t^*)\right] + y_2[F(t^*) - G^2(t^*)]^{1/2}\right\} = 0 , \qquad (2.14)$$

where $y_{1,2}$ are two independent Gaussian variables with zero average and standard deviation one, and $G(t)$ is defined as

$$G(t) = \left[\frac{D\mu(0)}{\mu(0)\tau - 1}\right]^{1/2} \int_0^t \exp\left[-\mu(0)s - \frac{vs^2}{2}\right]ds .$$
$$(2.15)$$

In practice, we have computed distributions of t^* by means of the following procedure: generate one (two) Gaussian deviate(s) for the external (internal) noise case; seek t^* as the solution of (2.11) or (2.14) for the particular value(s) of the random deviate(s); repeat the procedure many times, averaging until acceptable statistical quality has been achieved. Finally, t_{MFPT}^* is obtained in each case as the mean of the resultant distribution.

Equations similar to our (2.14) have been obtained by TSM (their 3.2, 3.3, and 3.4) for the external noise case and for $\tau = 0$. In the limit $\beta \ll 1$ and $z \gg 1$, TSM were also able to derive analytic expressions for the average and the standard deviation of z: in our notation,

$$z = T^{1/2} , \qquad (2.16a)$$

$$(\Delta z)^2 = \tfrac{1}{4}T^{-1}\psi'(1) , \qquad (2.16b)$$

where $\psi'(x)$ is the polygamma function[21] and T is defined as

$$T = \ln\frac{\sqrt{\Pi}a}{2\beta\{1 + a\sqrt{\Pi}e^{a^2}[\text{erf}(a) + 1]\}} . \qquad (2.17)$$

For the range of parameters considered in the present paper, however, (2.16) cannot be applied because the conditions $\beta \ll 1$ and $z \gg 1$ are not fulfilled. It should be noted that the semianalytic treatment given above solves the problem of the inversion of equation (3.4) of TSM for the whole range of parameters where a MFPT approach is meaningful.

III. TESTS OF THE THEORY

A. Techniques used

The theory was tested by analog experiment and digital simulation. The basis of each of these techniques[23,24] has been discussed in detail elsewhere, so only the salient features in their present applications will be summarized here.

For the analog experiment,[23] a suitably time-scaled electronic circuit was built to model Eqs. (2.1)–(2.4); this is shown diagrammatically in Fig. 4. The time scaling

$t \rightarrow t'/\tau_1$ results in the velocity and noise intensity each being scaled as $v \rightarrow v'\tau_I$, $D \rightarrow D'/\tau_I$, where the primed parameters denote the quantities measured in the circuit. For all the results reported here $v = 0.0618$ and $\tau_I = 824$ μs. The stochastic forcing $\eta(t)$ was Gaussianly distributed and exponentially correlated with correlation time $\tau_n = 22$ μs; thus the circuit perceived the stochastic forcing to be white.

The operation of the circuit was essentially the same for both the internal and external noise cases and was briefly as follows. Using additional switching circuitry (not shown) the integrator was initialized to the value $x(0)$ while $\mu(t)$ was held constant at the value $\mu(0)$. A triggering pulse was then applied to the switching circui-

FIG. 3. Sections taken through the evolving distribution of Fig. 2, to clarify the differences between the ZMB and MFPT definitions of t^*. (a) Section giving the $P(x^2)$ distribution at the t^* defined by ZMB. (b) Section at x_{th}^2 giving the $P(t)$ distribution from which the MFPT definition of t^* is derived.
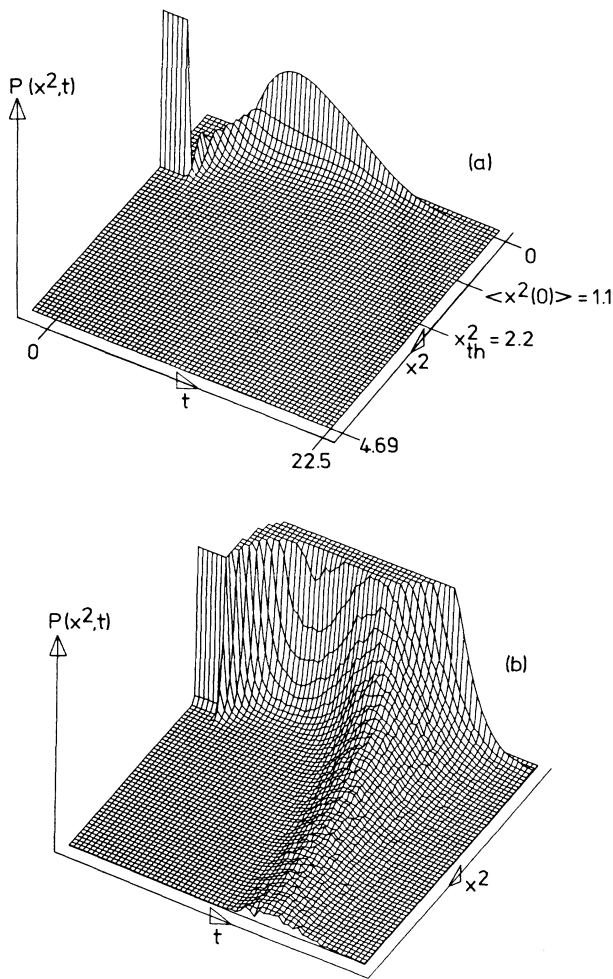

FIG. 2. The evolving distribution $P(x^2, t)$, as measured in an analog experiment for the case of external noise. The system is held at $x = x(0)$ until $t = 0$, at which time noise is applied and the sweep of μ simultaneously initiated according to Eq. (2.2). Both (a) and (b) represent the same set of data, but the vertical scale in (b) has been magnified compared to that in (a) in order to reveal more clearly the evolution at later times where $P(x^2, t)$ has become small because of the relatively high velocity.
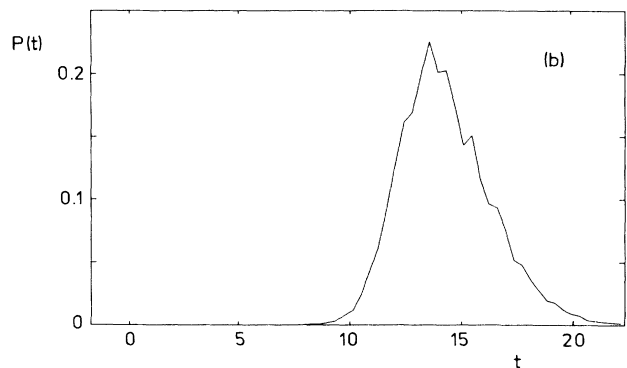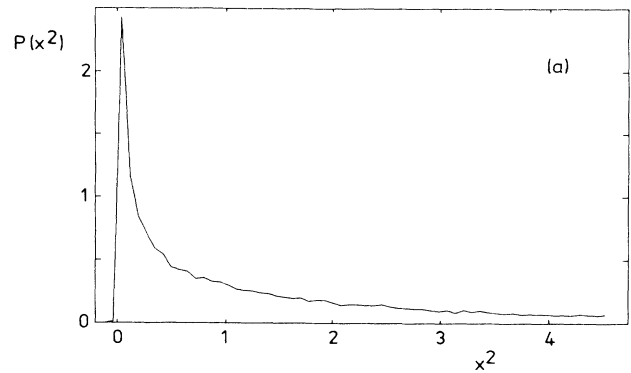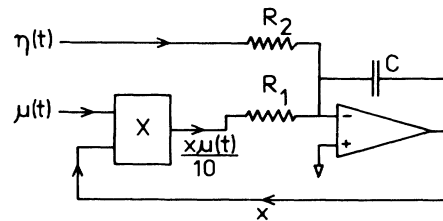

FIG. 4. Block diagram of the analog electronic circuit used to model the system described by Eqs. (2.1)–(2.4). Some additional circuitry employed to initialize the system, to provide the sweep of $\mu(t)$ according to (2.2) and to switch the noise input $\eta(t)$, when required, is not shown. For the case of external noise, the circuit was initialized at $x(0)$, and then released at $t = 0$ at which time the noise was simultaneously applied and the sweep of $\mu(t)$ was initiated; for the case of internal noise, the noise was applied continuously and the system was allowed to attain a stationary distribution centered on $x = 0$ prior to commencement of the sweep.

try which in turn applied a ramp to the $\mu(t)$ input and "released" the circuit, the noise was also applied at this instant [see Figs. 5(a) and 5(b)]. The triggering pulse was also applied simultaneously to the data processor (a Nicolet LAB-80) which, by means of ensemble averaging, constructed the statistical density of interest. The operation of the circuit for the internal noise case differed slightly, in that $\langle x(0)\rangle$ was always set equal to zero and the noise was also present during the initialization stage.

The algorithm used for the digital simulations has already been described.[25] It is an implicit algorithm for
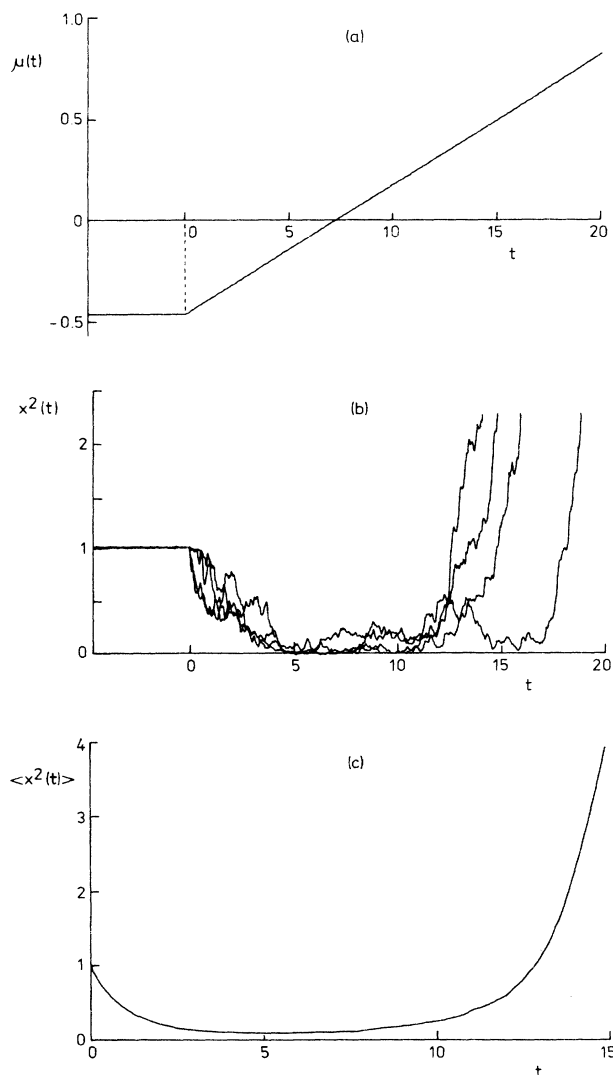

FIG. 5(a) The sweep of $\mu(t)$. Until $t=0$, μ is held at a fixed negative value; for $t>0$, it is swept linearly towards higher values. (b) Corresponding typical trajectories of $x^2(t)$ for the case of external noise. Until $t=0$, the circuit is held at a fixed value $x^2(0)$, at $t=0$, the system is released and the noise is applied simultaneously. (c) Ensemble average $\langle x^2(t)\rangle$ for a set of $x^2(t)$ trajectories like those shown in (b). Note that the abscissa scale differs from those of (a) and (b). The bifurcation time t^* for the ZMVB theory is given by the point at which $\langle x^2(t)\rangle$ crosses x_{th}^2.

colored noise, which allows for an integration time step much larger than the correlation time of the noise. The values of v and the correlation time of noise were chosen to be the same as the (scaled) quantities in the analog simulation. For the external noise case, x was set at a predetermined value and the noise was set at a value randomly chosen from the appropriate distribution. For the internal noise case, two random numbers were chosen and combined to give the initial value for x and for the noise, so Eq. (2.9) was satisfied. The integration time step was varied between 0.1 and 0.01, and the number of realizations per average was normally 4000 (consistency has been checked by repeating some runs with 10 000 realizations).

B. Results for external noise

The typical experimental measurement of the evolving distribution $P(x^2,t)$ shown in Fig. 2, which provides a valuable demonstration of the distinction between the different criteria for threshold crossing, has already been discussed. Some examples of the set of individual $x^2(t)$ trajectories from which Fig. 2 was derived are shown in Fig. 5(b), and the corresponding moment average $\langle x^2(t)\rangle$ is plotted in Fig. 5(c). From curves such as the latter, it is straightforward to determine t^* corresponding to the ZMVB theory, it being simply the time at which $\langle x^2(t)\rangle$ attains x_{th}^2. Some typical results obtained for a very small noise intensity ($b=0.01$) are plotted as circular data points in Fig. 6(a) for a number of different initial values $\mu(0)$; the data are plotted in terms of the reduced parameters z and a, defined by Eqs. (2.5).

For the MFPT definition of t^*, trajectories like those in Fig. 5(b) are analyzed in a different way: the time at which each *individual* trajectory attains x_{th}^2 is noted; and the corresponding distribution of passage times $P(t)$ is constructed, yielding a curve like that in Fig. 3(b) whose average yields the MFPT value of t^*. The square data points of Fig. 6(a) were derived in this way.

It is clear that for weak noise intensity, the precise definition adopted for t^* is unimportant and that all of the data are very well described by the ZMVB theoretical prediction, shown by the curve in Fig. 6(a). For stronger noise intensities the situation is, however, very different.

The results of Fig. 6(b) show what happens when the reduced noise intensity is increased by a factor of 10, to $b=0.1$, for two values of the threshold parameter α, defined by Eq. (2.5). The upper solid curve, the dashed curve, and the crosses, squares, and upward pointing triangles all correspond to $\alpha=2$; the lower solid curve and the downward pointing triangles correspond to $\alpha=1.03$. The solid curves represent the ZMVB theory in each case, and are clearly in excellent agreement with the triangular data points derived from the $\langle x^2(t)\rangle$ definition of t^*. The other data points, corresponding to the MFPT definition of t^*, are obviously not at all well described by the ZMVB theory. The analog experimental data (crosses) and the digital simulation results (squares) for $\alpha=2$ are, however, in excellent agreement both with each other and also with the calculation presented in Sec. II C, which is shown as a dashed curve. For $\alpha=1.03$, the

latter approach is inapplicable because of the increased importance of the static Kramers escape process, which makes it probable that the system will often reach x_{th}^2 while $V(x,t)$ still has a deep minimum and before the system has been swept into the unstable regime. It is for this same reason that the analog data for $\alpha=1.03$ (circles) have fallen below the ZMVB curve, whereas they would generally, for larger values of α, always exceed the ZMVB prediction.

The dot-dashed curve for $\alpha=2$ represents the deterministic ($D=0$) solution for external noise,

$$z =(a^2+\ln\alpha)^{1/2} , \tag{3.1}$$

which follows immediately from (2.11). It is interesting to note the existence of a range of a within which it lies below the dashed curve implying that, under these conditions, the effect of fluctuations is to *increase* the magnitude of the postponement. This at first sight astonishing result can be accounted for in terms of the shape of $P(t)$ as shown, for example, in Fig. 3(b): as D increases from zero, $P(t)$ broadens asymmetrically, developing a long tail at large t which then causes its average to fall beyond the position of its maximum. The digital and analog data of Fig. 6(b), although scattered, are not inconsistent with this conclusion.

C. Results for internal noise

The evolving distribution $P(x^2,t)$ measured for the case of internal noise is similar to the one for external noise shown in Fig. 2(a) except, of course, that the starting condition on the left-hand side of the figure is an equilibrium stationary distribution, rather than a singularity. The measured values of z are plotted as a function of a in Fig. 7 for two values of the reduced noise parameter β: the upper curves and data are for $\beta=0.1$, and the lower curve and data are for $\beta=0.35$. The crosses, representing analog experimental data for the $\langle x^2(t)\rangle$ definition of t^*, are in excellent agreement with the ZMVB theory (associated solid curve) for $\beta=0.1$. The data obtained from
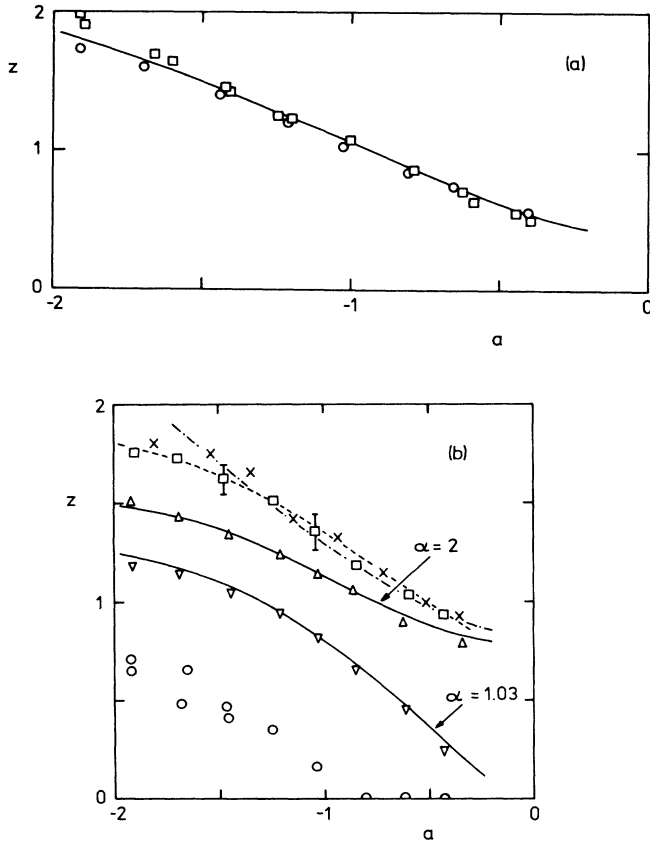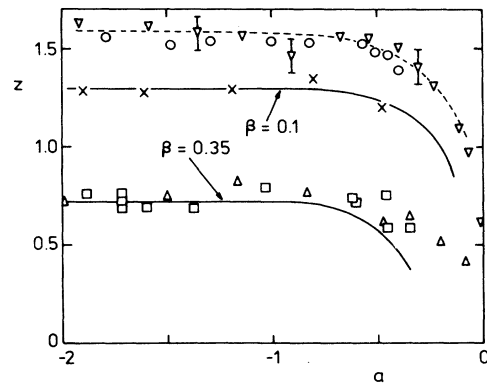

FIG. 6. Experiment and theory for the case of external noise. (a) The scaled bifurcation delay z plotted as a function of the scaled initial curvature of the potential a for $\alpha=1.2$ and very weak noise specified by $b=0.01$. The parameters z, a, α, and b are defined by Eqs. (2.5). The circular data points represent experimental values of z measured in the analog circuit using the $\langle x^2(t)\rangle$ definition of t^*; the square data points represent measurements based on the MFPT definition of t^*; and the curve is the ZMVB theory (Ref. 19). (b) A similar plot to that of (a) except that the noise is ten times stronger, with $b=0.1$. The triangular data points are experimental measurements based on the $\langle x^2(t)\rangle$ definition of t^* and the associated curves represent the ZMVB theory for $\alpha=1$ and 2, respectively. The crosses (analog experiment) and square (digital simulation) data points are based on the MFPT definition of t^*, for $\alpha=2$, and the dashed curve corresponds to the calculation described in Sec. II C. The circular data points represent analog experimental measurements for $\alpha=1$, where calculation by the method of Sec. II C is inapplicable. The dot-dashed curve represents the deterministic ($D=0$) solution for $\alpha=2$, given by Eq. (3.1).

FIG. 7. Experiment and theory for the case of internal noise. The scaled bifurcation delay z is plotted as a function of the scaled initial curvature of the potential a for two values of the noise parameter β. The definitions of z, a, and β are given in Eqs. (2.5). The crosses are experimental measurements based on the $\langle x^2(t)\rangle$ definition of t^* and the associated solid curve represents the ZMVB theory (Ref. 19) for $\beta=0.1$. The circular data (analog experiment) and point-down (digital simulation) are also for $\beta=0.1$, but are based on the MFPT definition of t^*; the dashed curve corresponds to the calculation described in Sec. II C. The square data (analog experiment) and point-up (digital simulation) for $\beta=0.35$ are also based on the MFPT definition of t^*; the fact that they are in reasonably good agreement with the ZMVB theory (associated solid curve) is believed to be coincidental (see text).

the MFPT definition of t^* are considerably higher: the circles are from the analog experiment and the triangles from the digital simulation; they are, however, in good agreement with each other and with the MFPT-based theory of Sec. II C, shown by the dashed curve. For $\beta = 0.35$, the latter theory is inapplicable for the reasons already stated. The fact that the MFPT analog (squares) and digital (triangles) data are quite well described by the ZMVB theory (lower solid curve) is probably coincidental: the data would generally be expected to fall above the ZMVB curve, but is here being "pulled down" by the static Kramers process, as already discussed. As already pointed out above, no direct comparison with (2.16) is possible. The excellent agreement between experiment and calculation for the MFPT definition of t^* with $\beta = 0.1$ strongly suggests, however, that for $\beta \ll 1$ and $z \gg 1$ (of relevance in real laser systems) the TSM approach should describe the experiments very well.

IV. CONCLUSION

In this paper we have used an analog electronic experiment to test the main results reported by ZMB for delayed bifurcations in a swept parameter system with additive white noise, for the cases of both internal and external noise. Their theory is, of course, exact and what the present experimental data have effectively confirmed is its applicability in the circumstances typical of a real physical system.

In addition, we have extended the discussion of ZMVB to encompass a different, and in some ways, more realistic definition of the characteristic bifurcation time t^*, based on the MFPT approach proposed by TSM (as opposed to ZMVB's moment average criterion). We have

shown how to calculate the MFPT-derived t^* in the limit that will most commonly apply to real swept parameter systems (in which contributions from the "static" Kramers escape process for $\mu < 0$ can be ignored); it reduces to the quantity calculated by TSM when $\beta \ll 1$ and $z \gg 1$. We have verified the calculation by analog experiment and digital simulation. Although the present experiments do not cover the parameter range where TSM were able to derive explicit theoretical expressions, we argue that their good agreement with the calculated MFPT bifurcation delay suggests that the TSM results should provide an excellent description of real laser systems where β is very small. We have demonstrated that the MFPT-derived bifurcation delay is generally larger than that defined by ZMVB, a result that is very much in accord with what would be expected from a consideration of the evolving distribution $P(x^2, t)$. For small thresholds relative to the starting value of $x^2(0)$ or $\langle x^2(0) \rangle$, however, the experiments clearly demonstrate that the MFPT-derived bifurcation delay can become smaller than the ZMVB value. The physical explanation is that the static Kramers escape process then allows $x^2(t)$ to exceed x_{th}^2 with significant probability even for $\mu < 0$, before inversion of the potential has occurred. We have also shown that (astonishingly) fluctuations can sometimes serve to increase the MFPT bifurcation delay.

*Also at Dipartimento di Fisica, Università degli Studi di Pisa, Piazza Torricelli 2, 56100 Pisa, Italy.

[1] W. Horsthemke and R. Lefever, *Noise-Induced Transitions: Theory and Applications in Physics, Chemistry and Biology* (Springer, Berlin, 1984).

[2] H. Risken, *The Fokker-Planck Equation* (Springer, Berlin, 1984).

[3] *Theory of Continuous Fokker-Planck Systems*, Vol. 1 of *Noise in Nonlinear Dynamical Systems*, edited by F. Moss and P. V. E. McClintock (Cambridge University Press, Cambridge, England, 1989); *Theory of Noise-Induced Processes in Special Applications*, Vol. 2 of *Noise in Nonlinear Dynamical Systems*, edited by F. Moss and P. V. E. McClintock (Cambridge University Press, Cambridge, England, 1989); *Experiments and Simulations*, Vol. 3 of *Noise in Nonlinear Dynamical Systems*, edited by F. Moss and P. V. E. McClintock (Cambridge University Press, Cambridge, England, 1989).

[4] P. Colet, M. San Miguel, J. Casademunt, and J. M. Sancho, Phys. Rev. A 39, 149 (1989); J. Casademunt, J. I. Jimenez-Aquino, and J. M. Sancho, Physica A (to be published).

[5] R. Roy, A. W. Yu, and S. Zhu, in Ref. 3, Vol. 3, Chap. 4.

[6] E. Arimondo, D. Hennequin, and P. Glorieux, in Ref. 3, Vol. 3, Chap. 5.

[7] W. Lange, in Ref. 3, Vol. 3, Chap. 6; F. Mitschke, C. Boden, and W. Lange, Phys. Rev. A 39, 3690 (1989).

[8] M. James, F. Moss, P. Hanggi, and C. Van den Broeck, Phys. Rev. A 38, 4690 (1988); J. M. Sancho and M. San Miguel, ibid. 39, 2722 (1989).

[9] J. Casademunt, J. I. Jimenez-Aquino, and J. M. Sancho (unpublished); J. Casademunt, J. I. Jimenez-Aquino, C. J. Lambert, R. Mannella, P. Martano, P. V E. McClintock, J. M. Sancho, and N. G. Stocks (unpublished).

[10] P. Mandel and T. Erneux, Phys. Rev. Lett. 53, 1818 (1984); T. Erneux and P. Mandel, Phys. Rev. A 30, 1893 (1984); P. Mandel and T. Erneux, J. Stat. Phys. 48, 1059 (1987).

[11] M. Lefebvre, D. Dangoisse, and P. Glorieux, Phys. Rev. A 29, 758 (1984); T. Midivaine, D. Dangoisse, and P. Glorieux, Phys. Rev. Lett. 55, 1989 (1985).

[12] D. K. Kondepudi, F. Moss, and P. V. E. McClintock, Physica 21D, 296 (1986); D. K. Kondepudi, in Ref. 3, Vol. 2, Chap. 10.

[13] G. Broggi, A. Colombo, L. A. Lugiato, and P. Mandel, Phys. Rev. A 33, 3635 (1986).

[14] L. A. Lugiato, G. Broggi, M. Merri and M. A. Pernigo, in Ref. 3, Vol. 2, Chap. 12.

[15] B. Morris and F. Moss, Phys. Lett. 118A, 117 (1986).

[16] R. Mannella, F. Moss, and P. V. E. McClintock, Phys. Lett. 120A, 11 (1987); Phys. Rev. A 35, 2560 (1987).

[17] L. Fronzoni, F. Moss, and P. V. E. McClintock, Phys. Rev. A 36, 1492 (1987).

[18]W. Sharpf, M. Squicchiarini, D. Bromley, C. Green, J. R. Tredicce, and L. M. Narducci, Opt. Commun. **63**, 344 (1987).

[19]C. Van den Broeck and P. Mandel, Phys. Lett. A **122**, 36 (1987); H. Zeghlache, P. Mandel, and C. Van den Broeck, Phys. Rev. A **40**, 286 (1989).

[20]M. C. Torrent and M. San Miguel, Phys. Rev. A **38**, 245 (1988).

[21]*Handbook of Mathematical Functions*, edited by M. Abramowitz and I. A. Stegun (Dover, New York, 1970).

[22]This point was given particular emphasis by F. T. Arecchi at the NATO Advanced Research Workshop on Noise and Chaos in Nonlinear Dynamical Systems, Turin, 1989.

[23]P. V. E. McClintock and F. Moss, in Ref. 3, Vol. 3, Chap. 9.

[24]R. Mannella in Ref. 3, Vol. 3, Chap. 7.

[25]R. Mannella and V. Palleschi, Phys. Rev. A (to be published).